Talanta 82 (2010) 687–692

Contents lists available at ScienceDirect

Talanta

journal homepage: www.elsevier.com/locate/talanta

Direct colorimetric visualization of mercury (Hg^{2+}) based on the formation of gold nanoparticles

Aiping Fan [a], Ying Ling [b], Choiwan Lau [a], Jianzhong Lu [a,*]

[a] School of Pharmacy, Fudan University, 826 Zhangheng Road, Sanghai, 201203, China
[b] School of Phmarceutical Science and Technology, Tianjin University, 92 Weijin Road, Tianjin, 300072, China

ARTICLE INFO

Article history:
Received 12 February 2010
Received in revised form 12 May 2010
Accepted 14 May 2010
Available online 21 May 2010

Keywords:
Gold nanoparticle
Mercury
colorimetric detection
$HAuCl_4$
NH_2OH

ABSTRACT

It is critical to be able to detect and quantify Hg^{2+} ions under aqueous conditions with high sensitivity and selectivity. The technique presented herein provides a direct way for simple colorimetric visualization of Hg^{2+} ions in aqueous solution, based on the formation of gold nanoparticles through the Hg^{2+} catalyzed $HAuCl_4/NH_2OH$ reaction. The outstanding selectivity and sensitivity result from the well-known amalgamation process that occurs between mercury and gold. The entire procedure takes less than 20 min. The limit of detection (2 ppb) shows excellent potential for monitoring ultralow levels of mercury in water samples.

1. Introduction

Mercury is a toxic element that exists in metallic, inorganic, and organic forms [1]. Mercuric ion (Hg^{2+}), one of the inorganic forms of mercury, exists mostly in surface water due to its high water solubility. Mercury ion shows strong affinity for the ligands containing S atom and thus causes the blocking of sulphydryl groups (-SH) of proteins and enzymes. Long-term exposure to high levels of mercury can lead to a variety of adverse health effects such as damage to the brain, nervous system, immune system and many other organs [2–4]. Therefore, it is critical to be able to detect and quantify Hg^{2+} under aqueous conditions with high sensitivity and selectivity.

There are various classical methods described in the literature for mercury detection. These include atomic absorption spectrometry (AAS) [5,6], atomic fluorescence spectrometry (AFS) [7], inductively coupled plasma mass spectrometry (ICPMS) [8,9], and reversed-phase high-performance liquid chromatography [10], which are powerful techniques for the determination of Hg^{2+}. Their excellent performance, however, is achieved at the expenses of expensive instrumentation and time-consuming sample preparation and preconcentration procedures. Hence, the interest in swapping instrumental analytical tools with suitable, selective, sensitive and low cost Hg^{2+} ion sensors has been increasing. Various sensor systems for the detection of Hg^{2+}, based upon organic chromophores or fluorophores [11–15], conjugated polymers [16,17], oligonucleotides [18,19], DNAzymes [20], proteins [21], thin films [22] and nanoparticles [23–25] have been reported. Optical sensors that do not require any special instrumentation are particularly attractive for the visual detection of Hg^{2+}. Several optical sensors have been developed for the detection of Hg^{2+} [12,23,26–32]. For example, Mirkin et al. [33] recently reported colorimetric detection of Hg^{2+} in aqueous media using DNA-functionalized gold nanoparticles (Au NPs). Xue et al. [34] developed a one-step colorimetric detection of Hg^{2+} by making use of DNA-Au NPs and thymine-Hg^{2+}-thymine coordination chemistry. Although such optical sensors are simpler than conventional methods, most of them are either limited with respect to the sensitivity (current limit of detection $\approx$ 100 nM), selectivity, requirement of electronic heating unit, sophisticated synthesis of the probe materials, or not suitable for on-the-spot sample assays. Therefore, it should be highly desirable to develop a detection system that is not only sensitive and selective, but also simple, practical, and economical in its operation.

Herein, we report a simple and sensitive method for the one-step, label-free, colorimetric detection of Hg^{2+} at ppb level by a simple hydroxylamine reduction reaction. NH_2OH is thermodynamically capable of reducing Au^{3+} ions to bulk metal [35]. The color of the solution turns to red when Au NPs are formed in the $HAuCl_4/NH_2OH$ reaction. We found that $HAuCl_4/NH_2OH$ reaction could also be accelerated by Hg^{2+} ions. The speed of color change is increased with the increase of the concentration of Hg^{2+} ions.

---

[*] Corresponding author. Tel.: +86 21 51980058.
E-mail address: jzlu@shmu.edu.cn (J. Lu).

0039-9140/$ – see front matter © 2010 Elsevier B.V. All rights reserved.
doi:10.1016/j.talanta.2010.05.033

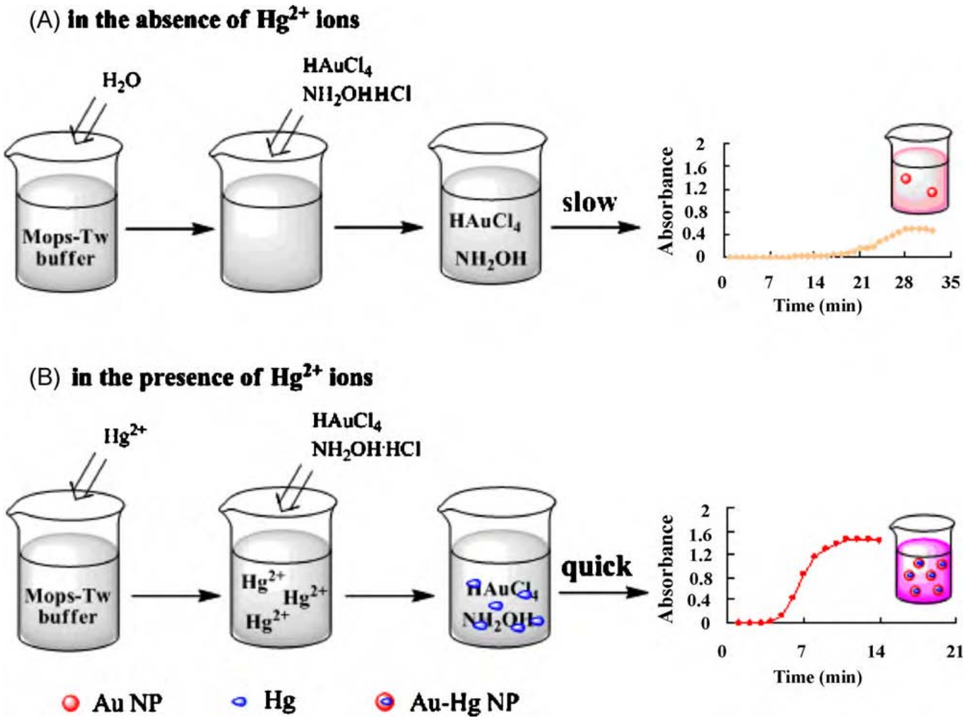

Scheme 1. Schematic representation of $HAuCl_4/NH_2OH$ reaction in the absence (A) and in the presence of Hg^{2+} ion (B).

Based on this phenomenon, a colorimetric method for the determination of Hg^{2+} in water samples is thus developed. The outstanding selectivity and sensitivity of the method provide a unique way to determine Hg^{2+} in water samples.

2. Experimental

2.1. Chemicals and apparatus

All chemicals were of analytical reagent grade and were used as received. The water was prepared using Milli-XQ equipment. Mops sodium salt was obtained from Alfa Aesar. 5 nm gold NPs were obtained from BB International. Tween 80 was purchased from Sigma-Aldrich. $HAuCl_4$, NH_2OH, $Hg(NO_3)_2$, sodium dodecylsulfate (SDS), cetyltrimethylammonium bromide (CTMAB), Triton X-100, Tween 20 and other reagents were purchased from Sinopharm Chemical Reagent Co. Ltd. Hg^{2+} ion stock solution (5 μM) was prepared by adding 50 μL of 0.1 mM $Hg(NO_3)_2$ into 950 μL of MOPS buffer (10 mM MOPS buffer containing 0.01% Tween 20, pH 7.0).

Absorption spectra, kinetic curves, calibration curve and interference tests were conducted on a Shimadzu UV-2410 UV/vis spectrophotometer. Other experiments, such as optimization of assay conditions, were monitored by a microplate reader (Thermo, MK3 Multiskan). Transmission electron microscopy (TEM) was performed on a transmission microscope (JEOL JEM-2011). ICPMS experiments were performed on Elan DRC-e.

2.2. The colorimetric detection of Hg^{2+}

In a typical experiment, 250 μL of 4 mM $HAuCl_4$ (adjusted to pH 3 by 4×10^{-2} M NaOH) and 500 μL of 9 mM $NH_2OH{\cdot}HCl$ were added into the reaction tube containing 250 μL of different concentration of Hg^{2+} ion. The final concentration of $HAuCl_4$ and NH_2OH were kept as 1 mM and 4.5 mM, respectively. The mixture was kept at room temperature for 16 min. The color change could be observed by the naked eye or quantified by a simple visual readout.

2.3. ICP-MS detection of Hg in Au NPs

The bulk volume was set to be 4 mL. 1 mL of desired concentration of Hg^{2+}, 1 mL of 4 mM of $HAuCl_4$ (adjusted to pH 3 by 4×10^{-2} M NaOH) and 2 mL of 9 mM of $NH_2OH{\cdot}HCl$ were mixed. The mixture was kept at room temperature for 16 min. Finally, the formed NPs were isolated by centrifugation, resuspended with water and recentrifuged. The centrifugation-resuspension-recentrifugation cycle was repeated twice. The red precipitate was resuspended in 4 mL of water. The ICP-MS determination of Hg in Au NPs was accomplished by Shanghai Institute of Measurement and Testing Technology.

3. Results and discussion

It is well known that NH_2OH is thermodynamically capable of reducing Au^{3+} to bulk metal, and the reaction is dramatically accelerated by Au surfaces [36]. Herein, we found that, even in the absence of Au surfaces, Hg^{2+} ions also have the ability to accelerate the formation of Au NP in $HAuCl_4/NH_2OH$ reaction, which can be used herein for the determination of Hg^{2+} ion. The principle of colorimetric detection of Hg^{2+} ions based on the formation of Au NPs is depicted in Scheme 1. The rate of particle growth is highly dependent on and proportional to the initial concentration of Hg^{2+} ions. The speed of color change is increased with the increase of the concentration of Hg^{2+}. Based on this phenomenon, a colorimetric method for the determination of Hg^{2+} in water samples is thus developed, which is simple, rapid, quantitative, and inexpensive.

3.1. Optimization of assay conditions

Several parameters were investigated systematically in order to establish optimal conditions for the direct colorimetric detection of mercury ions, including the type and concentration of surfactant,

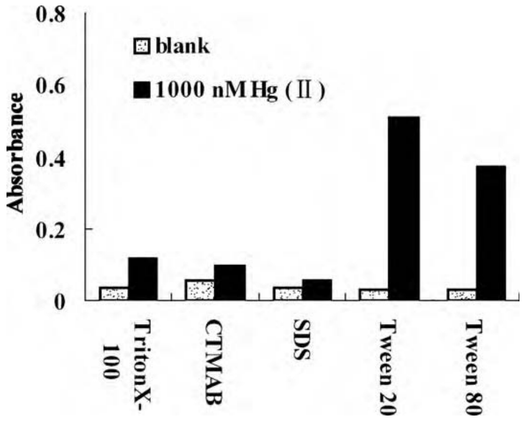

Fig. 1. Absorbance at 492 nm versus different kinds of surfactants. Experimental conditions: $HAuCl_4$, 0.5 mM; $NH_2OH{\cdot}HCl$, 4.5 mM; Hg^{2+} ions (in 10 mM Mops buffer containing 0.01% different kinds of surfactant, pH 7) 1000 nM; reaction time, 10 min.

the pH of mops buffer, the concentration of $HAuCl_4$ and $NH_2OH{\cdot}HCl$.

Metallic NPs are unstable and have a tendency to aggregate. Therefore, the use of stabilizer is very significant to prevent the aggregation and to maintain the stability of Au NPs in aqueous solution. Hence, as shown in Fig. 1, various kinds of surfactants including anionic surfactant (SDS), cationic surfactant (CTMAB) and nonionic surfactants (Triton X-100, Tween 20 and Tween 80) were studied. Nonionic surfactant was superior to anionic surfactant and cationic surfactant. A higher absorbance was obtained by using Tween 20 as stabilizer, which was then selected for further studies. Fig. 2 showed that the optimized concentration of Tween 20 was 0.01%. The pH of Mops buffer versus the absorbance was optimized as shown in Fig. 3. As the pH of Mops buffer increased, the absorbance increased quickly, indicating more Au NPs catalytically formed in the solution, and then decreased sharply due to a higher background. Hence, the pH of Mops solution was set at 7.0.

The influence of the concentration of $HAuCl_4$ was investigated as shown in Fig. 4. As the concentration of $HAuCl_4$ increased, the absorbance increased and reached a peak value at 1 mM, and at higher concentration the absorbance decreased. Hence, subsequent work employed 1 mM of $HAuCl_4$. As shown in Fig. 5, with increasing the concentration of NH_2OH, the absorbance increased sharply at the beginning, and reached maximum at 4.5 mM, then decreased slowly at higher concentration. Thus, 4.5 mM of NH_2OH was selected for the following studies.

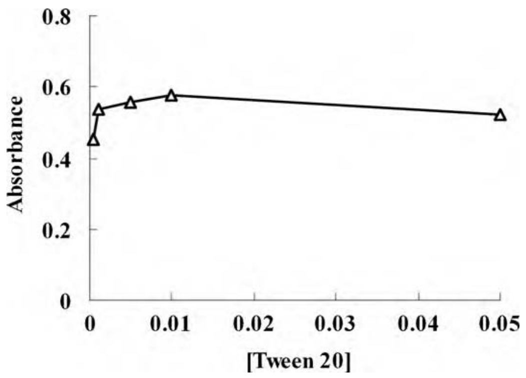

Fig. 2. Absorbance at 492 nm versus the concentration of Tween 20. Experimental conditions: Hg^{2+} ions (in 10 mM Mops buffer containing different concentration of Tween 20, pH 7), 1000 nM; other experimental conditions were the same as Figure 1.

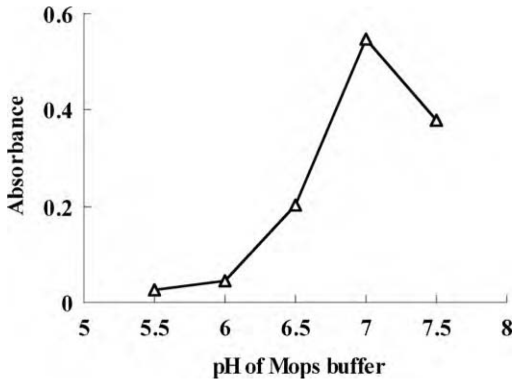

Fig. 3. Absorbance at 492 nm versus the pH of Mops buffer solution. Experimental conditions: Hg^{2+} ions (in different pH of 10 mM Mops buffer containing 0.01% Tween 20), 1000 nM; other experimental conditions were the same as Figure 1.

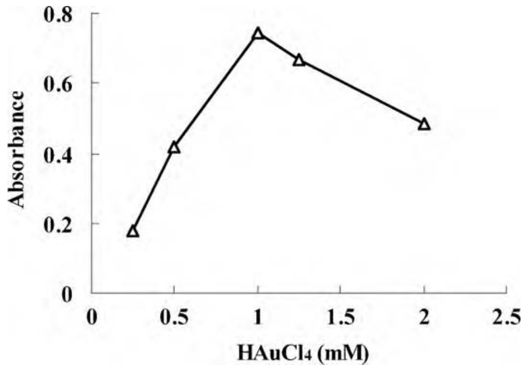

Fig. 4. Absorbance at 492 nm versus the concentration of $HAuCl_4$. Experimental conditions: different concentration of $HAuCl_4$, Hg^{2+} ions (in 10 mM Mops buffer containing 0.01% Tween 20, pH 7), 1000 nM; other experimental conditions were the same as Figure 1.

3.2. *Characterization of the formed Au NPs*

Fig. 6 displays the absorbance spectra for Au NPs which were formed in the Hg^{2+} catalyzed $HAuCl_4/NH_2OH$ reaction. The maximum absorption wavelength is 580 nm (Fig. 6A), while the maximum absorption wavelength for 5-nm Au NPs is 530 nm (Fig. 6B). Compared with 5-nm Au NPs, an observed red shift and broadening is obtained for the Au NPs formed in Hg^{2+} catalyzed $HAuCl_4/NH_2OH$ reaction, which indicates that large Au NPs are

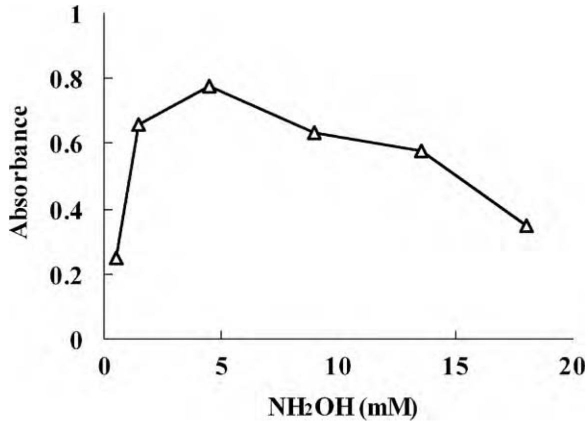

Fig. 5. Absorbance at 492 nm versus the concentration of NH_2OH. Experimental conditions: $HAuCl_4$, 1 mM; different concentration of $NH_2OH{\cdot}HCl$; other experimental conditions were the same as Figure 4.

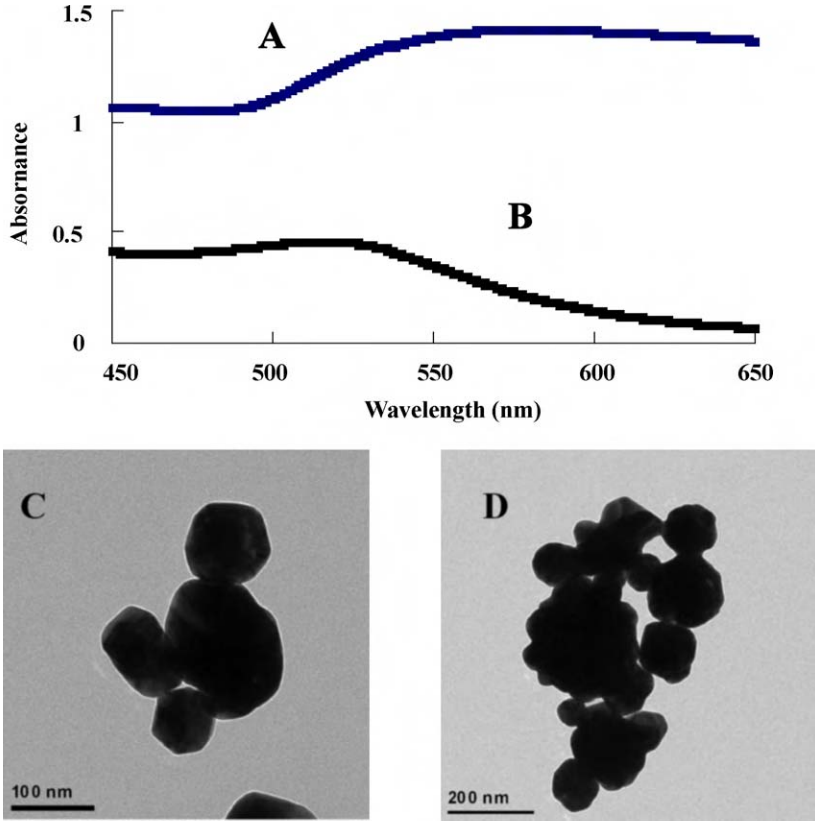

Fig. 6. Absorbance spectra (A) and TEM image (C, D) of Au NPs formed in Hg^{2+} catalyzed $HAuCl_4/NH_2OH$ reaction and absorbance spectra of 5 nm Au NPs (B). Experimental conditions for A, C and D: $HAuCl_4$, 1 mM; $NH_2OH{\cdot}HCl$, 4.5 mM; Hg^{2+} ions (in 10 mM Mops buffer containing 0.01% Tween 20, pH 7), 1000 nM; Reaction time, 16 min. Experimental conditions for B: 5 nm Au NPs, 41.5 nM.

formed in the solution. Fig. 6C and 6D display the transmission electron microscope (TEM) image of the Au NPs generated from Hg^{2+} catalyzed $HAuCl_4/NH_2OH$ reaction. The average diameter of the Au NPs is 119 ± 44 nm.

3.3. *Kinetic curve of the formation of Au NPs in the Hg^{2+} catalyzed $HAuCl_4/NH_2OH$ reaction*

The reaction rate of blank solution (Scheme 1A) without Hg^{2+} is much slower than that of sample solution containing Hg^{2+} (Scheme 1B). Figure 7 shows the absorbance changes observed at 580 nm by different concentrations of Hg^{2+} ions. Figure 7 shows that the plateau could not be reached at the same time in the presence of different concentrations of Hg^{2+} ions, i.e. the time required to reach the plateau was gradually decreased with the increase of the concentration of Hg^{2+} ions, indicating that the reaction rate is increased with the increase of the concentration of Hg^{2+} ion. To reach a plateau in absorbance at 580 nm, 29 min, 27 min, 24 min, 20 min, 12 min, and 11 min were needed for 0 nM, 10 nM, 100 nM, 250 nM, 1000 nM, and 2000 nM of Hg^{2+} ions, respectively. Besides the reaction rate, the absorbance at 580 nm, where plateau was reached, was also increased with the increase of Hg^{2+} concentration. However, the absorbance also decreased slightly after the plateau was reached. Hence, for a broad range of Hg^{2+} determination, the reaction time was set to be 16 min.

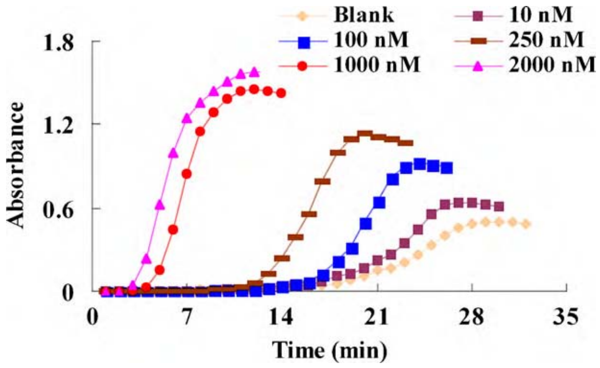

Fig. 7. Time-dependent absorbance changes at 580 nm upon analyzing different concentrations of Hg^{2+} ion. Experimental conditions: different concentrations of Hg^{2+} ions (in 10 mM MOPS buffer containing 0.01% Tween 20, pH 7); other experimental conditions were the same as Figure 6A. Recorded at 1-min intervals.

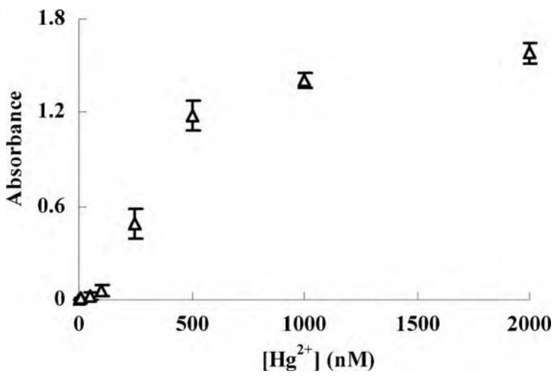

Fig. 8. Absorbance at 580 nm versus different concentrations of Hg^{2+} ions. Experimental conditions were the same as Figure 6A.

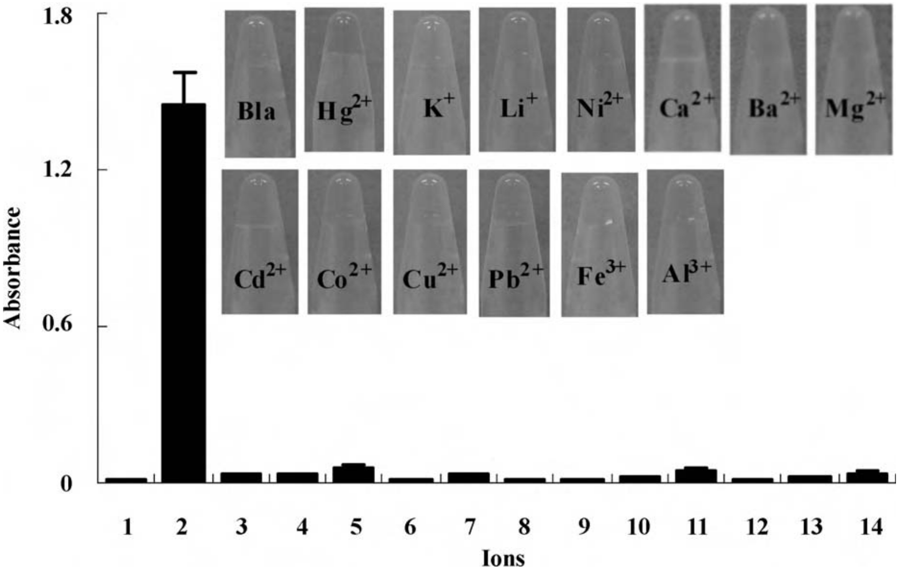

Fig. 9. Selectivity of the analysis of Hg^{2+} ions by the method depicted in Scheme 1. 1: Blank, 2: Hg^{2+}, 3: K^+, 4: Li^+, 5: Ni^+, 6: Ca^{2+}, 7: Ba^{2+}, 8: Mg^{2+}, 9: Cd^{2+}, 10: Co^{2+}, 11: Cu^{2+}, 12: Pb^{2+}, 13: Fe^{3+}, 14: Al^{3+}. The concentration of Hg^{2+} was 1 μM. Others were 100 μM. Other experimental conditions were the same as Figure 6A.

3.4. Sensitivity and selectivity

To evaluate the sensitivity of this method, different concentrations of Hg^{2+} (10, 50, 100, 250, 500, 1000, 2000 nM) from one stock solution were evaluated. As shown in Fig. 8, the absorbance proportionally correlated with the Hg^{2+} concentration. A calibration graph in the concentration range of 10-1000 nM showed a linear correlation ($R^2 = 0.907$) between the concentration of Hg^{2+} and the absorbance at 580 nm, represented by $I = 0.0016C + 0.0244$. The LOD under the optimal experimental condition was found to be 10 nM (2 ppb).

Moreover, we investigated the specificity of this assay for metal ions. 13 different kinds of metal ions (K^+, Li^+, Ni^+, Ca^{2+}, Ba^{2+}, Mg^{2+}, Cd^{2+}, Co^{2+}, Cu^{2+}, Pb^{2+}, Fe^{3+}, Al^{3+} and Ag^+, each at 100 μM) were tested under the same experimental conditions as in the case of Hg^{2+} (at 1 μM). Remarkably, no color changes of the solutions were observed with metal ions including K^+, Li^+, Ni^+, Ca^{2+}, Ba^{2+}, Mg^{2+}, Cd^{2+}, Co^{2+}, Cu^{2+}, Pb^{2+}, Fe^{3+} and Al^{3+}, even at a 100-fold higher concentration than that of Hg^{2+} (photographs in Fig. 9). Ag^+ ions, which would precipitate in the presence of $NH_2OH{\cdot}HCl$, also did not interfere with the determination of Hg^{2+} ions. The absorbance at 580 nm was recorded by an UV/Vis spectrophotometer. The Hg^{2+} exhibited a 25-115-fold stronger signal than that of any of the other metal ions (Fig. 9), which indicated high selectivity of this method. Note also that methyl mercury, as a typical type of organic mercury, did not induce any obvious color change under the same experimental conditions. This indicated that only free Hg^{2+} could be detected by using this method and organic mercury could not be detected directly. It is well known that different types of mercury including Hg, $Hg(OH)_2$, HgO, CH_3Hg^+ and CH_3HgCl, etc., can be transformed into Hg^{2+} ions by using a digestive method, and thus the proposed technique may offers great promise as a colorimetric detection method for the determination of total mercury.

3.5. The mechanism of the Hg^{2+} catalyzed $HAuCl_4/NH_2OH$ reaction

We assumed that, even in the absence of Au^{3+}, Hg^{2+} could also be reduced by NH_2OH, which induced the transformation of Hg^{2+} ions to liquid Hg. The equation could be described as $2HgCl_2 + 2NH_2OH \rightarrow 2Hg(l) + N_2O + H_2O + 4HCl$ and $HAuCl_4 + 2NH_2OH \rightarrow Au(s) + N_2O + H_2O + 4HCl$. In the presence of liquid Hg, two probable mechanisms of action should be considered: nucleation, or amalgamation between Au and Hg, or both, which accelerate the formation of Au NPs in solution. The equation could be described as $Hg(l) + 3Au(s) \rightarrow Au_3Hg$ and $2Hg(l) + Au(s) \rightarrow AuHg_2(l)$. Hg should be encapsulated inside or bind outside of the formed Au NPs. To classify the theory that liquid Hg takes part in the formation of Au NPs, we determined the amount of Hg in the Au NPs after the hydroxylamine reduction reaction by ICP-MS. The actual and theoretical amounts of Hg have good correlation with $R^2 = 0.9745$. About 30-40% of Hg is reduced and encapsulated inside or bind outside of the Au NPs. There are three possible reasons for the remaining portion of Hg^{2+}. First, the NH_2OH/Hg^{2+} reduction reaction was not complete and the unreacted Hg^{2+} ions were discarded in the washing step. Second, tiny liquid Hg particles may

Table 1
Comparison of optical methods for mercury detection.

Methods	Specific materials	Detection limit	Time	Ref
Fluorescence (FL)	Porphyrin dimer	0.52 μM	Real-time	[37]
FL	Gold NPs and Rhodamine 6G	0.06 nM	10 min	[24]
FL	DNA, gold NPs and OliGreen	25 nM	70 min	[38]
FL	TOTO-3 and DNA	0.6 ppb	15 min	[15]
UV-Vis	Gold NPs and DNA	250 nM	10 min	[39]
UV-Vis	Ruthenium complexes	20 ppb	2 min	[40]
Scanmetric	Gold NPs and DNA	2 ppb	≈2 h	[33]
Hyper Rayleigh Scattering	MPA-Hcys-PDCA modified gold NPs	5 ppb	6-7 min	[28]
UV-Vis	$HAuCl_4/NH_2OH$	10 nM (2 ppb)	15-20 min	Our method

be not encapsulated inside the Au NPs and lost during the washing step. Third, the liquid Hg may transform into vapor Hg and volatize into air.

3.6. Preliminary analysis of Hg^{2+} in water samples

To test the potential of our gold nanoparticle-based method for the analysis of Hg^{2+} in environmental samples, a water sample was collected from Jingye Lake on the campus of Tianjin University. The sample was first filtered through a 0.22 μm membrane to remove soil and other particles, and then tested by the proposed technique. No color change was observed in this water sample, indicating that Hg^{2+} ions were not found in this water sample. Then, the water samples were spiked with Hg^{2+} ions at different concentration levels, the recoveries of 20, 100, and 500 nM Hg^{2+} were $106.2 \pm 7.2\%$, $94.7 \pm 1.8\%$ and $66.8 \pm 2.6\%$, respectively. Therefore, the proposed method is attractive for monitoring low levels of mercury in water samples.

4. Conclusions

A colorimetric method for the label-free, sensitive, and highly selective determination of Hg^{2+} using a simple $HAuCl_4/NH_2OH$ reduction reaction is presented. This method is enzyme-free and does not require any specialized equipment. The concentration of Hg^{2+} can be determined by the naked eye assay and an UV/Vis spectrophotometer. Compared with previous methods (Table 1), this direct colorimetric technique offers advantages in four aspects: (1) one does not need to use any DNA or fluorescent dyes to probe Hg^{2+} ion in solution; (2) it is highly selective and sensitive; (3) it takes only 15-20 min to find out the concentration of Hg^{2+} ion in aqueous solution; and (4) only a low-cost absorbance device is needed for detection of Hg^{2+} ions, which make the technology very attractive for mobile and point-of-care. Our experimental results reported here open up a new possibility of rapid, easy, and reliable way for the determination of Hg^{2+} in water samples.

Acknowledgment

We acknowledge financial support from National Natural Science Foundation of China (20975026), Shanghai Key Basic Research Program (08JC1402600) and the Research Fund for the Doctoral Program of Higher Education (20090071110056).

References

[1] F.A. Cotton, G. Wilkinson, C.A. Murillo, M. Bochmann, Advanced Inorganic Chemistry, 6th ed., John Wiley & Sons, New York, 1999.
[2] H.H. Harris, I.J. Pickering, G.N. George, Science 301 (2003) 1203.
[3] J. Mutter, J. Naumann, R. Schneider, H. Walach, B. Haley, Neuroendocrinol. Lett 26 (2005) 439.
[4] W. Zheng, M. Aschner, J.F. Ghersi-Egea, Toxicol. Appl. Pharmacol 192 (2003) 1.
[5] Q. Yang, Q. Tan, K. Zhou, K. Xu, X.J. Hou, Anal. At. Spectrom 20 (2005) 760.
[6] C.J.D. Maciel, G.M. Miranda, D.P. de Oliveira, M.E. de Siqueira, J.N. Silveira, E.M.A. Leite, J.B.B. da Silva, Anal. Chim. Acta 491 (2003) 231.
[7] J.J.B. Nevadoa, R.C.R. Martín-Doimeadiosb, F.J.G. Bernardo, M.J. Moreno, J. Chromatogr. A 1093 (2005) 21.
[8] D. Karunasagar, J. Arunachalam, S. Gangadharan, J. Anal. At. Spectrom 13 (1998) 679.
[9] B.M. Fong, T.S. Siu, J.S. Lee, S. Tam, J. Anal. Toxicol. 31 (2007) 281.
[10] X. Yin, Q. Xu, X. Xu, J. Chin. Anal. Chem 23 (1995) 1168.
[11] S. Yoon, A.E. Albers, A.P. Wong, C.J. Chang, J. Am. Chem. Soc 127 (2005) 16030.
[12] C.C. Huang, H.T. Chang, Anal. Chem 78 (2006) 8332.
[13] H. Lu, Y. Tang, W. Xu, D. Zhang, S. Wang, D. Zhu, Macromol. Rapid Commun 29 (2008) 1467.
[14] J. Wang, B. Liu, Chem. Commun 39 (2008) 4759.
[15] C.K. Chiang, C.C. Huang, C.W. Liu, H.T. Chang, Anal. Chem 80 (2008) 3716.
[16] X. Liu, Y. Tang, L. Wang, J.Z. Song, C. Fan, S. Wang, Adv. Mater 19 (2007) 1471.
[17] I.B. Kim, U.H.F. Bunz, J. Am. Chem. Soc 128 (2006) 2818.
[18] S.J. Liu, H.G. Nie, J.H. Jiang, G.L. Shen, R.Q. Yu, Anal. Chem 81 (2009) 5724.
[19] Z.Q. Zhu, Y.Y. Su, J. Li, D. Li, J. Zhang, S.P. Song, Y. Zhao, G.X. Li, C.H. Fan, Anal. Chem 81 (2009) 7660.
[20] J. Liu, Y. Lu, Angew. Chem., Int. Ed 46 (2007) 7587.
[21] S.V. Wegner, A. Okesli, P. Chen, C. He, J. Am. Chem. Soc 129 (2007) 3474.
[22] K.Z. Brainina, N.Y. Stozhko, Z.V.J. Shalygina, Anal. Chem 57 (2002) 945.
[23] J.S. Lee, M.S. Han, C.A. Mirkin, Angew. Chem. Int. Ed 46 (2007) 4093.
[24] J. Chen, A. Zheng, A. Chen, Y. Gao, C. He, X. Kai, G. Wu, Y. Chen, Anal. Chim. Acta 599 (2007) 134.
[25] M. Rex, F.E. Hernandez, A.D. Campiglia, Anal. Chem 78 (2006) 445.
[26] T. Balaji, M. Sasidharan, H. Matsunaga, Analyst 130 (2005) 1162.
[27] D. Li, A. Wieckowska, I. Willner, Angew. Chem. Int. Ed 47 (2008) 3927.
[28] G.K. Darbha, A.K. Singh, U.S. Rai, E. Yu, H. Yu, P.C. Ray, J. Am. Chem. Soc 130 (2008) 8038.
[29] H. Wang, Y. Wang, J. Jin, R. Yang, Anal. Chem 80 (2008) 9021.
[30] E.M. Nolan, S.J. Lippard, J. Am. Chem. Soc 125 (2003) 14270.
[31] Y.K. Yang, K.J. Yook, J. Tae, J. Am. Chem. Soc 127 (2005) 16760.
[32] Y. Tanaka, S. Oda, H. Yamaguchi, Y. Kondo, C. Kojima, A. Ono, J. Am. Chem. Soc 129 (2007) 244.
[33] J.S. Lee, C.A. Mirkin, Anal. Chem 80 (2008) 6805.
[34] X. Xue, F. Wang, X. Liu, J. Am. Chem. Soc 130 (2008) 3244.
[35] G. Stremsdoerfer, H. Perrot, J.R. Martin, P. Clechet, J. Electrochem. Soc 135 (1988) 2881.
[36] K.R. Brown, M.J. Natan, Langmuir 14 (1998) 726.
[37] X.B. Zhang, C.C. Guo, Z.Z. Li, G.L. Shen, R.Q. Yu, Anal. Chem 74 (2002) 821.
[38] C.W. Liu, C.C. Huang, H.T. Chang, Langmuir 24 (2008) 8346.
[39] C.W. Liu, Y.T. Hsieh, C.C. Huang, Z.H. Lin, H.T. Chang, Chem. Commun 19 (2008) 2242.
[40] E. Coronado, J. Galan-Mascaros, C. Martı-Gastaldo, E. Palomares, J.R. Durrant, R. Vilar, M. Gratzel, Md.K. Nazeeruddin, J. Am. Chem. Soc 127 (2005) 12351.